Materials Research Proceedings 41 (2024) 120-126 https://doi.org/10.21741/9781644903131-13

# Influence of remelting lasing strategies on the fracture toughness of Hastelloy X manufactured by laser powder bed fusion

KELLER Clément[1,a *], VIEILLE Benoit[2,b] and DUCHAUSSOY Amandine[2,b]

[1]Laboratoire Génie de Production, Université de Technologie de Tarbes Occitanie Pyrénées, Université de Toulouse, Tarbes, France

[2]Groupe de Physique des Matériaux, Normandie Université, UMRCNRS 6634, Saint-Etienne du Rouvray, France

[a]clement.keller@enit.fr, [b]benoit.vieille@insa-rouen.fr, [c]amandine.duchaussoy@insa-rouen.fr

**Keywords:** Remelting, Fracture Toughness, Microstructure, Laser Powder Bed Fusion, Hastelloy X

**Abstract.** Additive manufacturing and, in particular, Laser Powder Bed Fusion Processes (LPBF), are known to generate non-equilibrium microstructures having a strong impact on the mechanical properties such as tensile of fatigue ones. To better control this impact, optimized lasing strategies can be employed. Among them, relasing or remelting ones have been proved to reduce the porosity and the surface roughness as well as to increase the ductility [1,2]. This particular manufacturing strategy seems, hence, to be a promising tool to modify the microstructure and mechanical properties of LPBF alloys and to optimize the mechanical properties. The objective of this study is to assess the influence of such relasing and its characteristics on the fracture toughness of Hastelloy X superalloys.

## Introduction

Laser powder bed-based processes are nowadays well employed in industry to generate parts with high degree of geometrical complexity. Those processes are then a powerful tool to generate lightweight structures and to limit the use of primary material in relation to the necessary reduction of greenhouse gaz emission. Nevertheless, due to its intrinsic characteristics, those processes generate thermal gradients and cooling rates as far as millions of K/m and K/s, respectively [1]. Consequently, the produced alloys exhibit complex microstructures from morphological and crystallographical texture to dendrite structures and nano-oxides [2]. Other defects such as lack-of-fusion, keyholes, residual stresses or high surface roughness are also observed for AM materials [3].

The mechanical properties of those LPBF materials are generally modified compared to their conventionally produced counterparts (forging, casting, rolling) [3]. In tension, if the process parameters are correctly set up, mechanical properties of many alloy families are generally higher than for others manufacturing processes [4]. In fatigue, even after surface roughness removal and residual stresses relieve, the endurance limit is still lower for AM compared to cast [5].

In order to optimize the microstructure and reduce material defects, remelting strategies have been proposed in literature. Using such remelting, a many folds microstructure modification has been observed. Such modification affects the grain size distribution [6], the surface roughness [7], the porosity [7] as well as the dendrite size [8]. Consequently, an increase in mechanical properties in tension affecting the yield stress [8, 9], the ultimate tensile strength [8, 9] and the ductility has been reported [8]. Those results reveal the great potential for such on-line treatments which can be applied in the entire part or only locally where improved microstructure and mechanical properties are needed.

Nevertheless, those remelting strategies have not been extensively characterized for fatigue or fracture toughness improvements which are key properties for an industrial use of many LPBF parts. The objective of this study is, hence, to focus on the effect of remelting on fracture toughness of superalloy Hastelloy X (HX) produced by laser powder bed fusion. This study is based on two previous works made by the authors: one the capacity of remelting/relasing to improve the mechanical properties in tension [8] and the second one on the fracture toughness of Hastelloy X produced by LPBF without remelting [10].

**Experimental procedures**

Laser powder bed fusion manufacturing was carried out using a M400 EOS machine located in the Volum-e company in France. Hastelloy X powder was provided by Auber and Duval and is characterized by an average particle diameter of about 30 µm. The chemical composition followed the standard for this material. To investigate the role played by the laser remelting on the fracture toughness of HX, three manufacturing strategies were considered to produce mechanical samples. A first conventional strategy without remelting was employed to generate reference data on mechanical properties. This strategy is called HX_ref in the following paragraphs and parameters related to this production are summarized in table 1. Two others manufacturing strategies with remelting/relasing (a first laser scan melts the powder and a second scan interacts with the solidified material) were also employed based on a previous work [8]. The first one, denoted HX_R100 corresponds to a remelting with the exact same parameters as the reference one, in particular the laser power which is kept as 100% of the nominal value. The second one - HX_R60 - is similar with, nevertheless, a laser power set up to 60% of the nominal value employed for the two previous strategies. This 60% relasing power was found to provide the best compromise between yield stress and ductility in tension for vertical samples [8]. For the two relasing/remelting strategies the laser follows the exact same path for the two scans.

*Table 1: Laser Power Bed Fusion manufacturing parameters (SLM EOS M400-4)*

| Laser power [W] | Laser scanning speed [mm/s] | Hatch distance [mm] | Powder layer thickness [µm] | Layer to layer angle misorientation [°] |
|---|---|---|---|---|
| 288 | 960 | 0.11 | 40 | 67 |

To estimate the material fracture toughness, ASTM E1820 standard was applied [11]. It consists in investigating the crack propagation in Single Edge Notched samples submitted to bending (SENB tests). The fracture toughness is then estimated by means of the critical strain energy release $J_{Ic}$ which is computed from the crack tip opening displacement as well as from mechanical properties in tension. Consequently, in order to estimate fracture toughness values as accurately as possible, both bending samples and tensile tests ones were produced using the three manufacturing strategies described above. As the mechanical behavior of this material produced by LPBF has been proved to be anisotropic, two sample configurations, vertical (V) and horizontal (H) were manufactured. In the specific case of fracture toughness samples, the crack is initially oriented parallel and perpedicular to the lasing plane for the V and H configuration, in the order given. For the tensile samples, they were extracted from a 20x20x80 mm block using EDM. Each test was repeated three times. Figure 1 illustrates the sample geometry for the two mechanical tests. Sample thickness for tension is about 1 mm.

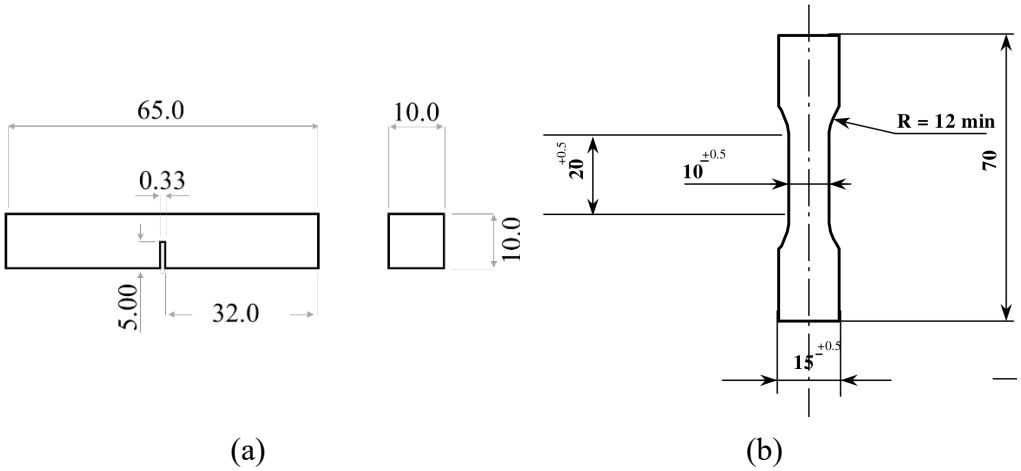


*Figure 1: Illustration of the sample geometry for: (a) single edge notched bending tests and (b) tensile tests. All dimensions are in mm.*

Tensile tests were conducted in strain rate control ($10^{-4}$ $s^{-1}$) mode using a conventional extensometer whereas the SENB tests were carried out in displacement-controlled mode (1 mm/min). The digital image monitoring of the crack propagation and the data analysis method for computing $J_{Ic}$ are described in a previous work [10]. Digital images were binarized and analyzed using a Scilab script enabling the crack length to be measured as well as the Crack Tip Opening Displacement (CTOD) at any time of the loading [10].

**Results and discussion**

Figure 2 illustrates the tensile behavior of the H and V samples manufactured using the three LPBF strategies. Different trends can be observed. On the one hand, despite different lasing strategies, for each direction (H or V), the tensile curves remain similar, in particular in the vertical direction. It can be also observed that the HX_R100 samples exhibit lower strain hardening, as already reported for cylindrical samples in a previous study [8]. On the other hand, regardless the lasing strategy, samples manufactured horizontally exhibit larger flow stress than the vertical direction. Nevertheless, this anisotropy seems to be lower for the samples manufactured with relasing, especially the HX_R100 strategy. Due to the low thickness of the tensile samples, fracture occurs without necking when maximal stress is reached.

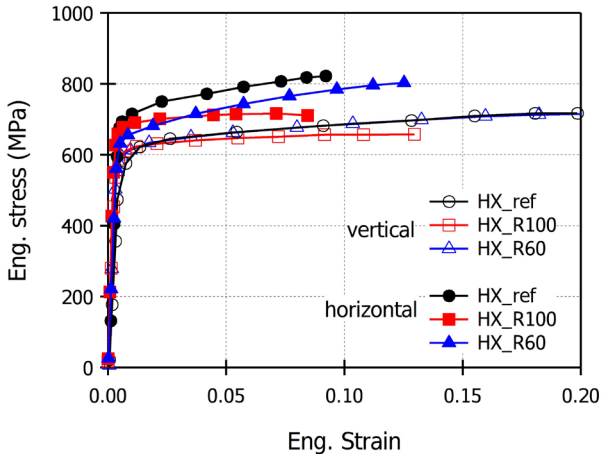


*Figure 2. Engineering tensile curves of Hastelloy X samples manufactured with or without relasing in the horizontal or vertical configurations.*

The bending curves representing the flexural force versus displacement are depicted in figure 3(a) and figure 3(b) for the vertical and horizontal configuration, respectively. The different curves are similar with a first stage characterized by an increasing force related to the elastoplastic behavior and further hardening of the material. The second stage characterizes the crack propagation associated with a significant decrease in the flexural force. The crack initiation is expected to occur during the end of stage I but not necessarily at the maximal force. As for tensile conditions, the mechanical behavior in bending is more anisotropic for the horizontal direction compared to the vertical one. It can be also observed that plasticity in the HX_R60appears for lower forces than for the other two configurations.

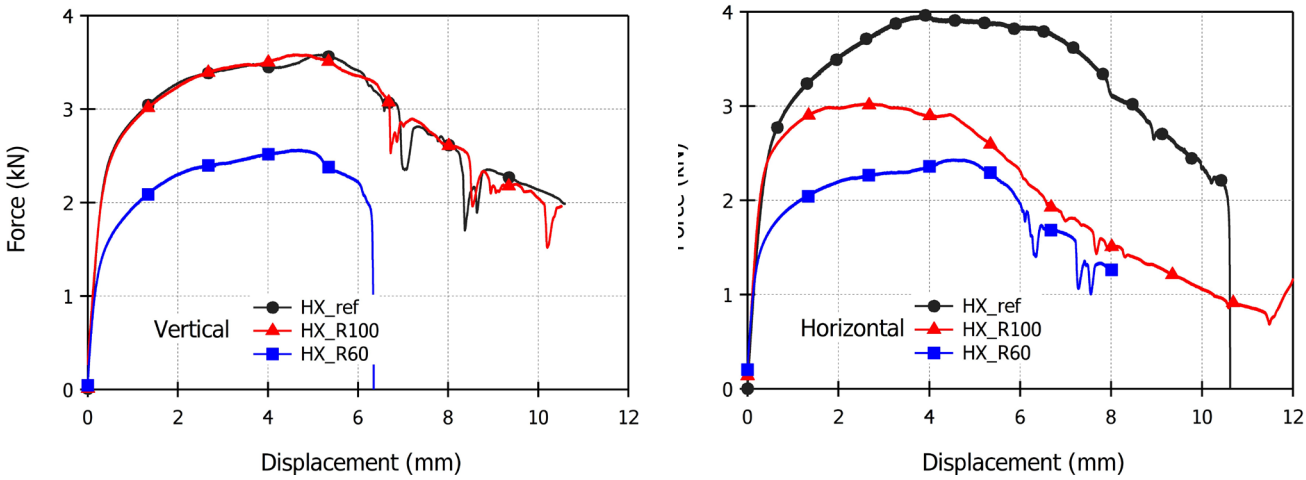


(a) (b)

*Figure 3: Bending curves for the single edged notch Hastelloy samples manufactured with the three LPBF configurations with or without relasing: (a) vertical and (b) horizontal configurations.*

In order to precisely estimate the fracture toughness at initiation, the Crack Tip Opening Displacement $\delta$ was computed during the test by means of a CCD camera allowing the crack propagation to be monitored. This parameter is computed according to eq. 1 [10]:

$$\delta = \delta_{elastic} + \delta_{plastic} = \frac{K^2(1-\nu^2)}{2\sigma_0 E} + \frac{r_p(W-a_0)V_p}{r_p(W-a_0)+a_0} \quad (1)$$

In this equation $K$ is the stress intensity factor relative to the specimen, the initial crack geometry and load at initiation, $\nu$ is the Poisson ratio, $E$ is the Young modulus, and $r_p$ is the plastic rotational factor ($r_{p,SENB} \approx 0.44$) whereas $W$ and $a_0$ correspond to the sample width and the initial crack length, respectively. $\sigma_0$ represents the yield stress and $V_p$ the crack mouth displacement at initiation measured by image analysis.

The critical strain energy release can be hence computed from the value $\delta$ at initiation as well as the yield stress and ultimate tensile stress provided by the tensile tests for all manufacturing conditions as detailed in eq. 2:

$$J_{Ic} = m\left(\frac{\sigma_0+\sigma_{UTS}}{2}\right)\delta \quad (2)$$

In that equation, $\sigma_0$ and $\sigma_{UTS}$ represent the yield stress and ultimate tensile strength, respectively and $m$ is a parameter depending on the crack geometry and on the material's strain hardening which can be empirically estimated using ASTM E1290 [12] and eq. 3:

$$m = 1.221 + 0.793(a_0/W) + 2.751n - 1.418(a_0/W)n \quad (3)$$

n is, in that case, the strain hardening exponent which can be computed using eq. 4 following ASTM E1290 standard. $R$ represents $R = \sigma_{UTS}/\sigma_0$ computed using tensile data.

$$n = 1.724 - 6.098/R + 8.326/R^2 - 3.965/R^3 \quad (4)$$

Using the actual values of the bending sample geometry, the tensile data as well as the Crack Tip Opening Displacement at initiation, the fracture toughness $J_{IC}$ can be estimated in all configurations (vertical and horizontal), and for the three manufacturing strategies. Figure 4 illustrates the fracture toughness values for all configurations tested in this study. From these values, it turns that, considering the experimental scattering, the manufacturing strategy does not seem to significantly affect the fracture toughness at initiation in the vertical configuration. Besides, a slightly improved value of fracture toughness is exhibited for the relasing configuration with 60% of the nominal power in agreement with the increase in ductility already observed for the vertical configuration [8]. For the horizontal configuration, the relasing strategy has a major effect with a maximal value of $J_{IC}$ of about 1300 kJ.m$^{-2}$ for the standard manufacturing strategy. The value obtained for relasing strategies are about 1000 kJ.m$^{-2}$ which are lower than for the vertical configuration but still widely larger than for the cast (230 kJ.m$^{-2}$ [13]). One can also observed that the fracture toughness anisotropy almost disappeared for the HX_R100 configuration as also observed in figure 2 for tensile conditions.

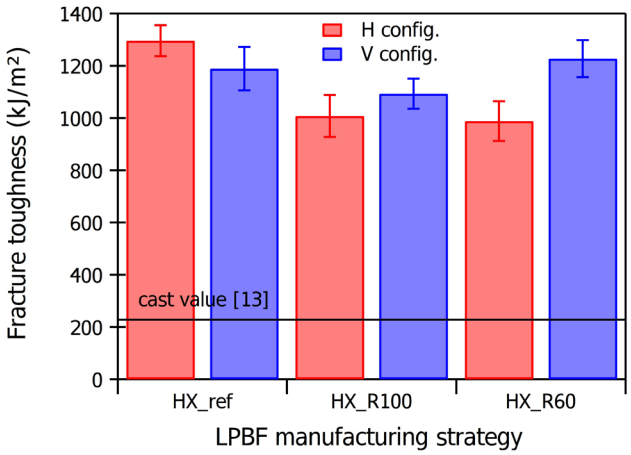


*Figure 4: Fracture toughness estimation for Hastelloy X samples manufactured with different LPBF strategies and building directions (vertical and horizontal).*

Following the conclusions of previous works conducted on Inconel 718 [14] and 316L [15] printed by LPBF, the horizontal configuration is generally detrimental to the fracture toughness when the crack propagates alongside the building direction due to the preferential intergranular mode involved by the elongation of the grains with respect to this direction. Similar mechanisms could be operating in the case of the Hastelloy X for the relasing strategies. Microstructural observation must be performed to understand the origin of the lower fracture toughness in the horizontal configuration for both relasing strategies compared to the reference case.

## Conclusions

Based on the characterization of tensile and fracture behavior, results from this study show that remelting affects the overall mechanical properties with, in particular:

- A decrease in the flow stress with remelting in the horizontal configuration.
- A detrimental effect on fracture toughness for horizontal configuration (crack propagating perpendicularly to the lasing planes) independently of the relasing strategy. Values are nevertheless five times larger than the one reported for cast.
- A slightly beneficial effect on fracture toughness for low relasing power (60%) in the vertical configuration (crack lying in the lasing planes).

A detailed analysis on the microstructure is then needed to better understand the origin of such effect of the remelting strategy.

## References

[1] M.V. Pantawane, Y-H. Ho, S. S. Joshi, N. B. Dahotre, Computational Assessment of Thermokinetics and Associated Microstructural Evolution in Laser Powder Bed Fusion Manufacturing of Ti6Al4V Alloy, Scientific reports, 10 (2020) 7579. https://doi.org/10.1038/s41598-020-63281-4

[2] Y.M. Wang, T. Voisin, J.T. McKeown, J. Ye, N. P. Calta, Z. Li, Z. Zeng, Y. Zhang, W. Chen, T.T. Roehling, R.T. Ott, M.K. Santala, P.J. Depond, M.J. Matthews, A.V. Hamza, T. Zhu, Additively manufactured hierarchical stainless steels with high strength and ductility. Nature Mater 17 (2018) 63–71. https://doi.org/10.1038/nmat5021

[3] T. DebRoy, H.L. Wei, J.S. Zuback, T. Mukherjee, J. W. Elmer, J. O. Milewski, A. M. Beese, A. Wilson-Heid, A. De, W. Zhang, Additive manufacturing of metallic components – Process, structure and properties. Progress in Materials Science 92 (2018) 112–224. https://doi.org/10.1016/j.pmatsci.2017.10.001

[4] S. Gorsse, C. Hutchinson, M. Gouné, R. Banerjee, Additive manufacturing of metals: a brief review of the characteristic microstructures and properties of steels, Ti-6Al-4V and high-entropy alloys. Science and Technology of Advanced Materials 18 (2017) 584–610. https://doi.org/10.1080/14686996.2017.1361305

[5] O. Karaka, F. B. Kardes, P. Fito, F. Berto, An overview of factors affecting high cycle fatigue of additive manufacturing metals, FFEMS 46 (2023) 1649-1668. https://doi.org/10.1111/ffe.13967

[6] S. Griffiths, M. Rossell, J. Croteau, N. Vo, D. C. Dunand, C. Leinenbach, Effect of laser rescanning on the grain microstructure of a selective laser melted al-mg-zr alloy, Materials Characterization 143 (2018) 34–42. https://doi.org/10.1016/j.matchar.2018.03.033

[7] E. Yasa, J. Deckers, J.-P. Kruth, The investigation of the influence of laser re-melting on density, surface quality and microstructure of selective laser melting parts, Rapid Prototyping Journal 17 (5) (2011) 312–327. https://doi.org/10.1108/13552541111156450

[8] C. Keller, M. Mokhtari, B. Vieille, H. Briatta, P. Bernard, Influence of a rescanning strategy with different laser powers on the microstructure and mechanical properties of Hastelloy X elaborated by powder bed fusion, Mat. Sci. Eng. A803 (2021) 1404754. https://doi.org/10.1016/j.msea.2020.140474

[9] Z. Xiao, C. Chen, Z. Hu, H. Zhu, X. Zeng, Effect of rescanning cycles on the characteristics of selective laser melting of ti6al4v, Optics Laser Technology 122 (2020) 105890. https://doi.org/10.1016/j.optlastec.2019.105890

[10] B. Vieille, A. Duchaussoy, S. Benmabrouk, R. Henry, C. Keller, Fracture behavior of Hastelloy X elaborated by laser powder bed fusion: Influence of microstructure and building direction, Journal of Alloys and Compounds 918 (2022) 165570. https://doi.org/10.1016/j.jallcom.2022.165570

[11] ASTM E1820-01, Standard Test Method for Measurement of Fracture Toughness, ASTM International, West Conshohocken, PA, 2001.

[12] ASTM E1290-90. Standard test method for crack-tip opening displacement (CTOD) fracture toughness measurement. American Society for Testing and Materials; 1998

[13] K. Krompholz, E.D. Grosser, K. Ewert. Determination of J-integral R-curves for Hastelloyx X and Inconel 617 up to 1223K using the potential drop technique. Materialwissenschaft Und Werkstofftechnik (1982), 13, pp. 236-244. https://doi.org/10.1002/mawe.19820130704

[14] B. Vieille, C. Keller, M. Mokhtari, H. Briatta, T. Breteau, J. Nguejio, F. Barbe, M. Ben Azzouna, E. Baustert, Investigations on the fracture behavior of Inconel 718 superalloys obtained from cast and additive manufacturing processes, Mat. Sci. Eng, A790 (2020) 139666. https://doi.org/10.1016/j.msea.2020.139666

[15] E. De Sonis, S. Depinoy, P-F. Giroux, H. Maskrot, P. Wident, O. Hercher, F. Villaret, A-F. Gourgues-Lorezon, Microstructure – Toughness relationships in 316L stainless steel produced by laser powder bed fusion, Mat. Sci. Eng, A877 (2023) 145179. https://doi.org/10.1016/j.msea.2023.145179